

Nanostructures

DOI: 10.1002/anie.200602298

Nanofibers with Tunable Stiffness from Self-Assembly of an Amphiphilic Wedge–Coil Molecule***Jung-Keun Kim, Eunji Lee, and Myongsoo Lee**

Self-assembly of amphiphilic block molecules can lead to a variety of nanostructures, which include spherical micelles, vesicles, nanofibers, and tubes.^[1] Extensive efforts have thus been made toward the design of novel molecular architec-

[*] J.-K. Kim, E. Lee, Prof. M. Lee

Center for Supramolecular Nanoassembly and
Department of Chemistry
Yonsei University
Shinchon 134, Seoul 120-749 (Korea)
Fax: (+ 82) 2-393-6096
E-mail: mslee@yonsei.ac.kr

[**] This work was supported by the National Creative Research Initiative Program of the Korean Ministry of Science and Technology. We acknowledge the Pohang Accelerator Laboratory, Korea, for use of the synchrotron radiation source. E.L. thanks the Seoul Science Fellowship Program.



Supporting information for this article is available on the WWW under <http://www.angewandte.org> or from the author.

tures consisting of incompatible components that are able to assemble into nanostructures with desired functions. Among the nanostructures formed by self-assembly of designed molecules, a 1D fibrillar assembly has proved to be particularly interesting for applications such as nanowires and biomimetic macromolecules.^[2] The 1D structures with stimuli-responsive features are likely to further enhance their scope as intelligent materials. Although stimuli-responsive nanostructures have been extensively studied with spherical objects,^[3] switching of the properties triggered by external stimuli with 1D fibrillar objects remains challenging.^[4] In this context, we have been interested in the preparation of a stimulus-responsive 1D cylindrical assembly with tunable properties triggered by the solvent environment.

Herein, we report the formation of cylindrical micelles from the self-assembly of a wedge-coil block molecule, and reversible switching between rigid rodlike aggregates and flexible coil-like aggregates triggered by a change in solvent polarity (Figure 1). The wedge-coil molecule, **1**, that forms

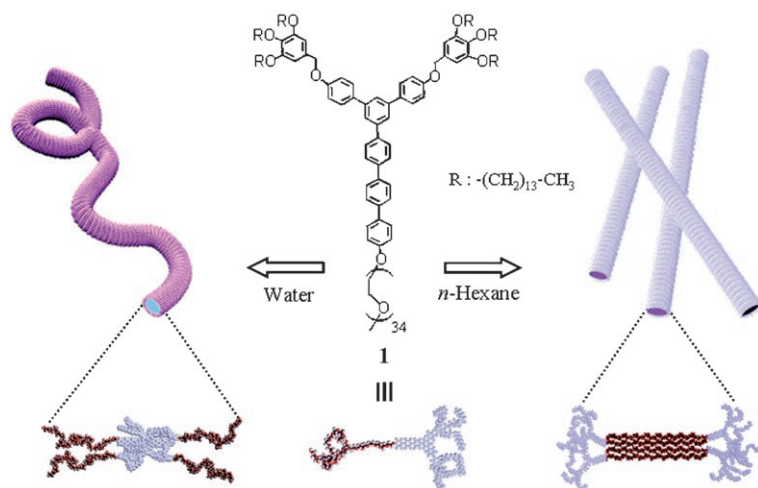


Figure 1. Schematic representation of the flexible coil-like and stiff rodlike nanofibers.

the cylindrical aggregates consists of a wedge-shaped rigid aromatic segment containing a tetradecyloxy periphery, and a flexible poly(ethylene oxide) (PEO) chain (degree of polymerization, DP = 34; volume fraction of PEO, $f_{\text{PEO}} = 0.43$), which are covalently linked at the apex of the wedge segment. The synthesis of the wedge-coil molecule was achieved in a stepwise fashion according to the procedures described previously.^[5] The resulting molecule was characterized by ¹H NMR spectroscopy, elemental analysis, gel-permeation chromatography, and MALDI-TOF mass spectrometry, and was shown to be in full agreement with the structures presented.

The wedge-coil molecule **1**, when dissolved in a solvent selective for one of the blocks, can self-assemble into an aggregate structure because of its amphiphilic characteristics. Dynamic light scattering (DLS) experiments were performed with **1** in water (0.01 wt%), a selective solvent for the PEO chains, and *n*-hexane (0.01 wt%), a selective solvent for the hydrophobic wedge segments, to investigate the aggregation

behavior. The wedge-coil molecule showed aggregation behavior in both water and *n*-hexane, as revealed by the autocorrelation functions (see Supporting Information). The angular dependence of the apparent diffusion coefficient (D_{app}) was measured because the slope is related to the shape of the diffusing species.^[6] The slopes measured in water and *n*-hexane were 0.033 and 0.025, respectively, consistent with the value predicted for nonspherical micelles with an elongated shape (0.03). The formation of cylindrical micelles in both solvents was further confirmed by the Kratky plots, which show a linear angular dependence on the scattered light intensity of the aggregates.^[7] A CONTIN analysis of the autocorrelation function in aqueous solution shows a broad peak corresponding to an average hydrodynamic radius (R_h) of approximately 138 nm. This result suggests the formation of highly flexible cylindrical micelles in aqueous solution.^[8] In contrast, a CONTIN size distribution analysis in *n*-hexane shows two sharp peaks corresponding to R_h values of 12 and 45 nm, characteristic of two relaxation modes as a result of the coupling of translational and rotational diffusion of rigid rodlike micelles.^[9]

Evidence for the formation of the cylindrical aggregates in both polar and apolar solvents was also provided by transmission electron microscopy (TEM) experiments (Figure 2). The micrographs negatively stained with an aqueous solution of uranyl acetate (2 wt%; Figure 2a) show highly curved cylindrical objects with a uniform diameter of about 15 nm, which indicates the formation of flexible coil-like nanofibers. To obtain more information on these nanofibers, we additionally performed TEM experiments with an ultramicrotomed film dried from aqueous solution (positively stained with RuO₄). The cross-sectional image of the fibers shows more stained dark aromatic domains surrounded by lighter PEO segments (Figure 2b).^[10a] The diameter of the core was measured as approximately 5 nm, which is the estimated

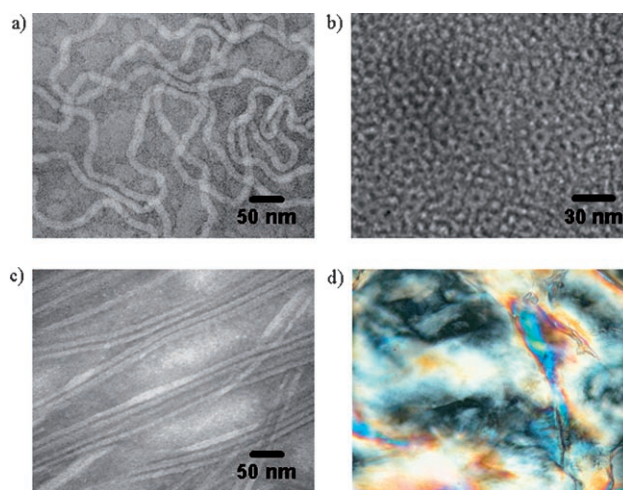


Figure 2. a) TEM image of nanofibers of **1** in aqueous solution (negatively stained with uranyl acetate); b) cross-sectional TEM image of nanofibers of **1** in aqueous solution (positively stained with RuO₄); c) TEM image of nanofibers of **1** in *n*-hexane solution (positively stained with RuO₄); and d) a representative optical polarized micrograph of the nematic phase in *n*-hexane solution.

length of an aromatic part together with a tetradecyl group (5.4 nm, by Corey–Pauling–Kultin (CPK) modeling). This result suggests that the core of the fiber formed from aqueous solution consists of an aromatic segment and tetradecyl groups, which are fully interdigitated with each other.

Similar to the aqueous solution, the wedge-coil block molecule in *n*-hexane was also observed to form cylindrical objects. However, the curvature of the cylindrical micelles formed in *n*-hexane is significantly different from that in water. The micrographs positively stained from RuO₄ showed bundles of the cylindrical aggregates aligned parallel to each other. These cylinders have lengths up to several micrometers and a uniform diameter of about 16 nm (Figure 2c). Notably, there is clear contrast between the periphery and center of the cylindrical object, which indicates that the cylinders consist of a light coil interior and dark aromatic exterior in *n*-hexane solution.^[10] Considering the extended molecular length (13.8 nm by CPK), the diameter of 16 nm indicates that the PEO chains within the core are fully interdigitated with each other. The formation of bundles of the micelles could be attributed to the existence of stiff rodlike micelles, consistent with the DLS results.

A rodlike shape with a high aspect ratio is a crucial prerequisite to form liquid-crystalline ordering,^[11] and thus the *n*-hexane solution was further investigated with polarized optical microscopy. As expected for stiff rodlike aggregates, the solution (8 wt %) is highly birefringent with a threadlike texture (Figure 2d), indicative of the formation of a lyotropic nematic liquid crystal. Evidence for the formation of rigid rodlike nanofibers is also provided by X-ray scattering experiments. In contrast to the small-angle X-ray scattering (SAXS) pattern of the aggregates formed from aqueous solution, which showed only a weak reflection (Figure 3a), the SAXS pattern of the dried liquid crystal formed from *n*-hexane solution showed a strong reflection corresponding to a spacing of 16.2 nm, thus demonstrating the presence of an ordered structure (Figure 3b). Notably, this dimension is consistent with the diameter determined from TEM.

These results demonstrate that the wedge-coil molecule self-assembles into highly flexible coil-like cylinders in polar solvents such as water, whereas stiff rodlike cylinders are formed in nonpolar solvents such as *n*-hexane. This remarkable contrast in stiffness of the cylindrical objects depending on solvent polarity can be understood by considering the packing arrangements of the molecular segments within the cylindrical core. In aqueous solution, the core of the cylindrical micelles consists of hydrophobic dendritic wedge segments, because water is a selective solvent for PEO.^[12] The bulky dendritic architecture of the hydrophobic part in the cylindrical core frustrates the crystallization process, which prevents the dense packing of the dendritic segments.^[13] As a result, this loose distribution of the hydrophobic segments in the cylindrical core leads to highly flexible cylindrical micelles.

In *n*-hexane solution, however, the micelles consist of a PEO core surrounded by hydrophobic wedge segments. Within the cylindrical domains, the hydrophilic chains with linear geometry crystallize to result in the dense packing of the core. This crystalline nature of the PEO segments within

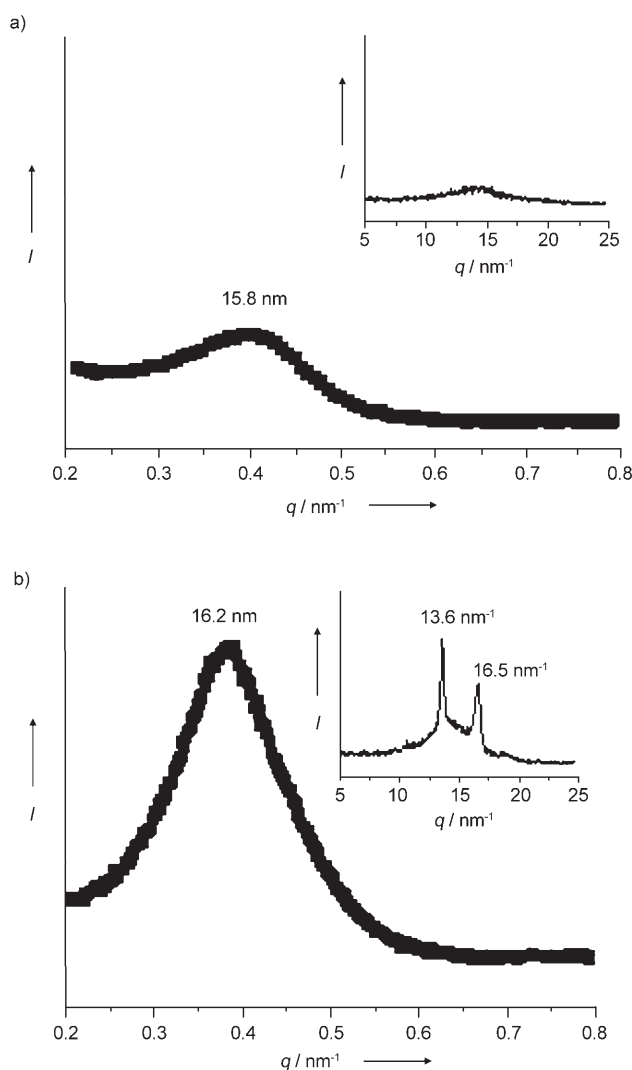


Figure 3. a) SAXS pattern of molecule 1 formed from aqueous solution (inset: wide-angle X-ray scattering (WAXS) pattern); and b) SAXS pattern of molecule 1 formed from *n*-hexane solution (inset: WAXS pattern).

the cylindrical core is reflected in wide-angle X-ray scattering (WAXS) measurements (Figure 3b, inset). The WAXS pattern of the dried liquid-crystal gel formed from *n*-hexane solution showed two sharp reflections, which indicate crystalline packing of the PEO segments within the domains.^[5] To further confirm the PEO packing within the cylindrical aggregates, FTIR spectroscopic experiments were performed because this technique has already been successfully used to investigate fundamental questions of PEO morphology.^[14] FTIR spectra corresponding to the CH₂ wagging mode, which is sensitive to the crystalline packing, are shown in Figure 4. The film cast from *n*-hexane solution showed two peaks at 1360 and 1343 cm⁻¹ (see Table 1), which contribute to modes in the crystalline phase of PEO. Upon exchange of the solvent to water, however, these peaks transformed into a single peak centered at 1350 cm⁻¹ which is assigned to amorphous PEO. These results together with the WAXS patterns demonstrate that the PEO core in hexane solution is

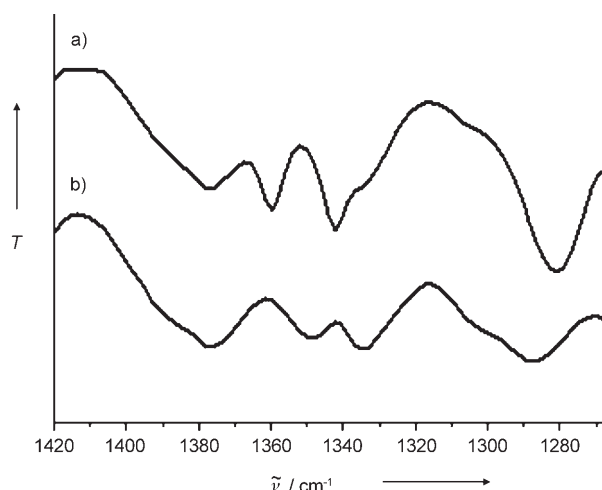


Figure 4. FTIR spectra of molecule **1** formed from a) *n*-hexane solution and b) aqueous solution in the 1270–1400 cm⁻¹ region.

Table 1: Frequencies and peak assignments of the FTIR bands of **1** at 1270–1400 cm⁻¹.

$\bar{\nu}$ [cm ⁻¹]		Assignment
1 in water	1 in <i>n</i> -hexane	
1377	1377	CH ₃ deformation
	1360	CH ₂ wag, C–C stretch
1350		
	1343	CH ₂ wag
1334	1334	ring C–C stretch
1305	1305	ring C–H in-plane bending, ring C–C stretch
1288		
	1280	CH ₂ twist

a highly ordered crystalline material, which is responsible for the formation of stiff rodlike cylindrical fibers.

The notable feature of the amphiphilic wedge–coil block molecule investigated here is its ability to self-assemble into cylindrical nanofibers in both polar and nonpolar solvents. Remarkably, as the solvent polarity changes from water to *n*-hexane, the resulting nanofibers change from a highly flexible coil-like character to a stiff rodlike nature. This switching in the stiffness of the nanofibers in response to solvent polarity is attributed to the structural inversion of the cylindrical core from bulky dendritic segments with an amorphous nature to crystallizable linear PEO segments. This structural inversion opens up the possibility of using this block molecule for applications such as encapsulation and/or release of molecules of interest, stimuli-sensitive templating media, and smart surfaces.

Received: June 8, 2006

Revised: July 27, 2006

Published online: September 29, 2006

Keywords: amphiphiles · nanostructures · self-assembly · solvent effects · supramolecular chemistry

- [1] a) S. Förster, T. Plantenberg, *Angew. Chem.* **2002**, *114*, 712–739; *Angew. Chem. Int. Ed.* **2002**, *41*, 688–714; b) S. Jain, F. S. Bates, *Science* **2003**, *300*, 460–464; c) D. E. Discher, A. Eisenberg, *Science* **2002**, *297*, 967–973; d) W.-Y. Yang, E. Lee, M. Lee, *J. Am. Chem. Soc.* **2006**, *128*, 3484–3485; e) T. Shimizu, M. Masuda, H. Minamikawa, *Chem. Rev.* **2005**, *105*, 1401–1444; f) M. Antonietti, C. Göltner, *Angew. Chem.* **1997**, *109*, 944–964; *Angew. Chem. Int. Ed. Engl.* **1997**, *36*, 910–928.
- [2] a) I. Manners, *Science* **2001**, *294*, 1664–1666; b) J. D. Hartgerink, E. Beniash, S. I. Stupp, *Science* **2001**, *294*, 1684–1688; c) T. Koga, M. Higuchi, T. Kinoshita, N. Higashi, *Chem. Eur. J.* **2006**, *12*, 1360–1367; d) A. Aggeli, I. A. Nyrkova, M. Bell, R. Harding, L. Carrick, T. C. B. McLeish, A. N. Semenov, N. Boden, *Proc. Natl. Acad. Sci. USA* **2001**, *98*, 11857–11862; e) W. Meier, C. Nardin, M. Winterhalter, *Angew. Chem.* **2000**, *112*, 4747–4750; *Angew. Chem. Int. Ed.* **2000**, *39*, 4599–4602.
- [3] a) M. Lee, S.-J. Lee, L.-H. Jiang, *J. Am. Chem. Soc.* **2004**, *126*, 12724–12725; b) J. Rodríguez-Hernández, S. Lecommandoux, *J. Am. Chem. Soc.* **2005**, *127*, 2026–2027; c) Z. Hu, A. M. Jonas, S. K. Varshney, J.-F. Gohy, *J. Am. Chem. Soc.* **2005**, *127*, 6526–6527; d) D. R. Vutukuri, S. Basu, S. Thayumanavan, *J. Am. Chem. Soc.* **2004**, *126*, 15636–15637; e) E. R. Gillies, T. B. Jonsson, J. M. J. Fréchet, *J. Am. Chem. Soc.* **2004**, *126*, 11936–11943.
- [4] a) H.-J. Kim, J.-H. Lee, M. Lee, *Angew. Chem.* **2005**, *117*, 5960–5964; *Angew. Chem. Int. Ed.* **2005**, *44*, 5810–5814; b) J.-H. Ryu, M. Lee, *J. Am. Chem. Soc.* **2005**, *127*, 14170–14171; c) D. J. Hill, M. J. Mio, R. B. Prince, T. S. Hughes, J. S. Moore, *Chem. Rev.* **2001**, *101*, 3893–4011; d) M. Barboiu, J.-M. Lehn, *Proc. Natl. Acad. Sci. USA* **2002**, *99*, 5201–5206; e) J. Xu, E. R. Zubarev, *Angew. Chem.* **2004**, *116*, 5607–5612; *Angew. Chem. Int. Ed.* **2004**, *43*, 5491–5496.
- [5] a) J.-K. Kim, M.-K. Hong, J.-H. Ahn, M. Lee, *Angew. Chem.* **2005**, *117*, 332–336; *Angew. Chem. Int. Ed.* **2005**, *44*, 328–332; b) S. Peleshanko, J. Jeong, V. V. Shevchenko, K. L. Genson, Yu. Pikus, M. Ornatska, S. Petrasch, V. V. Tsukruk, *Macromolecules* **2004**, *37*, 7497–7506.
- [6] a) M. Schmidt, W. H. Stockmayer, *Macromolecules* **1984**, *17*, 509–514; b) J. Massey, K. N. Power, I. Manners, M. A. Winnik, *J. Am. Chem. Soc.* **1998**, *120*, 9533–9540.
- [7] J. Boersma, *J. Chem. Phys.* **1981**, *74*, 6989–6990.
- [8] J. F. Gohy, B. G. G. Lohmeijer, A. Alexeev, X.-S. Wang, I. Manners, M. A. Winnik, U. S. Schubert, *Chem. Eur. J.* **2004**, *10*, 4315–4323.
- [9] a) M. Al-Hussein, B. G. G. Lohmeijer, U. S. Schubert, W. H. de Jeu, *Macromolecules* **2003**, *36*, 9281–9284; b) R. Pecora, *J. Chem. Phys.* **1968**, *48*, 4126–4128.
- [10] a) J. Bae, J.-K. Kim, N.-K. Oh, M. Lee, *Macromolecules* **2005**, *38*, 4226–4230; b) M. Lee, B.-K. Cho, K. J. Ihn, W.-K. Lee, N.-K. Oh, W.-C. Zin, *J. Am. Chem. Soc.* **2001**, *123*, 4647–4648.
- [11] S. M. Yu, V. P. Conticello, G. Zhang, C. Kayser, M. J. Fournier, T. L. Mason, D. A. Tirrell, *Nature* **1997**, *389*, 167–170.
- [12] This finding was also confirmed by dye encapsulation experiments (see Supporting Information).
- [13] The amorphous nature within the cylindrical micelles formed in aqueous solution was confirmed by X-ray scattering experiments that showed only a broad halo in the wide-angle range (see Figure 3a, inset).
- [14] a) M. A. K. L. Dissanayaket, R. Frech, *Macromolecules* **1995**, *28*, 5312–5319; b) Y. Su, J. Wang, H. Liu, *Langmuir* **2002**, *18*, 5370–5374.